Supplement of Biogeosciences, 21, 2143–2158, 2024
https://doi.org/10.5194/bg-21-2143-2024-supplement

Biogeosciences Open Access EGU

Supplement of

Multi-model comparison of trends and controls of near-bed oxygen concentration on the northwest European continental shelf under climate change

Giovanni Galli et al.

Correspondence to: Yuri Artioli (yuti@pml.ac.uk)

S1 Ensemble validation

Since climate models do not necessarily reproduce the climate system's phase, a direct point-to-point comparison with observations is not appropriate, conversely, comparing model- and observation-based climatologies is a more appropriate validation practice (Sellar et al., 2020; Yool et al., 2021). Model results are assessed against the North Sea Biogeochemical Climatology (NSBC) dataset (Hinrichs et al., 2017). This dataset covers the region 47° - 65 °N and 15 °W - 15 °E (roughly the NWES minus the Armorican Sea) for the period 1960-2014 and collates observational data for multiple physical and biogeochemical variables. Data are quality controlled and come in the form of optimally interpolated 3D-fields.

Model-based climatologies were computed over the 1990-2005 period as 2005 is the last year of historical simulation within the CMIP5 models. As validation metrics we considered normalised bias, nbias, and normalised unbiased root mean squared distance, nurmsd (Jolliff et al., 2009);

$$nbias = \frac{\mu_m - \mu_r}{\sigma_r} \quad \text{(eq. S1)}$$

$$nurmsd = \frac{sign\left(\sigma_m - \sigma_r\right)}{\sigma_r} \sqrt{\frac{1}{N}\sum_{i=1}^{N}\left(\left(m_i - \mu_m\right) - \left(r_i - \mu_r\right)\right)^2} \quad \text{(eq. S2)}$$

Where μ and σ are mean and standard deviation of model (m) and reference (r, observation) fields. nbias and nurmsd were computed for each sub-basin of the NEWS (Fig. 1). N is the number of grid points in each sub-basin. The sign() operator in nurmsd provides information on whether the model's σ is larger (nurmsd>0) or smaller (nurmsd<0) than than the reference field's. Normalisation of both metrics (division by σ_r) aims at facilitating the comparison across ensemble members and variables.

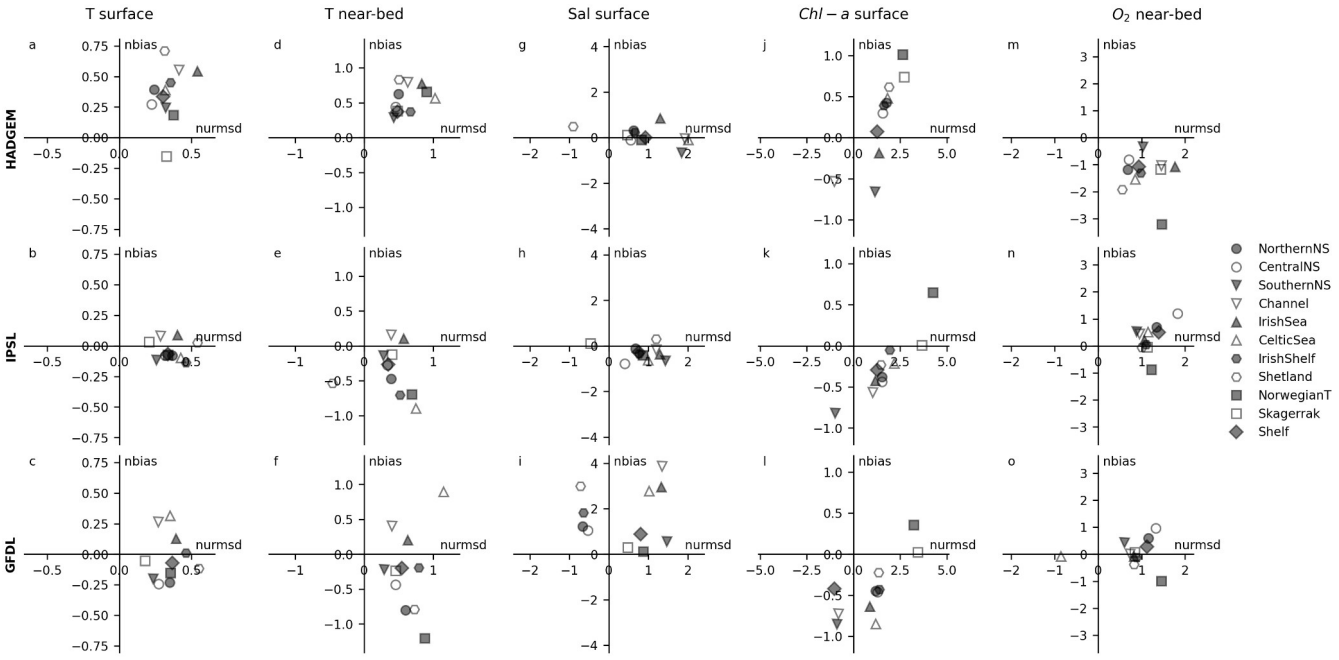

Fig. S1. Validation results. Plots show normalised bias (nbias) vs normalised unbiased root mean squared distance (nurmsd) for selected variables in the three ensemble members and in different model subdomains. A perfect fit would sit at the origin (0.0, 0.0).

Validation results are shown in Fig. S1. HADGEM overestimates both surface and near-bed temperature over most of the domain (nbias up to 0.75σ and nurmsd higher than the other members). IPSL and GFDL perform better with nbias generally within ±0.25σ and nurmsd generally within 0.5σ for surface values but greater for bottom values. Of the two IPSL performs better, especially for surface values. Surface salinity (here analysed because of its relatiaon to stratification) is well represented in both the HADGEM and IPSL, with nbias, nurmsd values generally within ±0.5σ. GFDL instead overestimates surface salinity with nbias between 3 and 4σ in the Channel, Irish Sea, Shetland and Celtic Sea. Surface chlorophyll-a (here considered as a proxy for primary production) is fairly well represented in all models (nbias values always within ±1σ). On average HADGEM overestimates surface chlorophyll, while IPSL and GFDL underestimate it, although this is not consistent across all subdomains. nurmsd values range approximately between 1 and 5σ, but normally within 2.5σ, and comparable across models. Near-bed oxygen is underestimated in HADGEM (nbias generally within -2σ, nurmsd between 0.5 and 2σ). IPSL and GFDL perform better, with positive nbias around ±1σ and nurmsd between 0.5 and 2σ. Finally, nurmsd values are generally positive, meaning that the models' σ is almost always larger than that of the NSBC dataset (observations).

S2. Relation between metrics of oxygen change decomposition

In this study we used the following decomposition of oxygen change where O_2 is dissolved oxygen, $O_{2,sat}$ is the saturation concentration and SS the saturation state, and the subscripts t and t0 are the final and initial time points of the interval over which the difference Δ is calculated:

$$\Delta O_2 = SS_{t0}\,\Delta O_{2,sat} + O_{2,sat,t0}\,\Delta SS + \Delta O_{2,sat}\,\Delta SS \quad \text{(eq. S3)}$$

Alternatively oxygen change can be partitioned using the classical Apparent Oxygen Utilisation (AOU) metric (Duteil et al. 2013), which is defined as,

$$AOU = O_{2,sat} - O_2 = O_{2,sat}\left(1 - SS\right) \quad \text{(eq. S4)}$$

hence,

$$\Delta O_2 = \Delta O_{2,sat} - \Delta AOU \quad \text{(eq. S5)}$$

since $O_2 = SS\ O_{2,sat}$, ΔAOU can be further decomposed,

$$\Delta AOU = \left(1 - SS_{t0}\right)\Delta O_{2,sat} + O_{2,sat,t0}\,\Delta\left(1 - SS\right) + \Delta O_{2,sat}\,\Delta\left(1 - SS\right) \quad \text{(eq. S6)}$$

The last terms in eq. S3 and eq. S6 are second order terms, they are strictly negligible when dealing with infinitesimals but not necessarily so for differentials. However, they usually are small compared to the other terms therefore we will neglect them from here on.

By substituting eq. S6 in eq. S5 and combining with eq. S3, and remembering that $-\Delta(1 - SS) = \Delta SS$, we get:

$$SS_{t0}\,\Delta O_{2,sat} + O_{2,sat,t0}\,\Delta SS = \Delta O_{2,sat} + \left(SS_{t0} - 1\right)\Delta O_{2,sat} + O_{2,sat,t0}\,\Delta SS \quad \text{(eq. S7)}$$

By rearranging the first two terms on the right we obtain the first term on the left, hence the two decompositions are equivalent.

Furthermore, from eq. 6 we can re-write ΔAOU as,

$$\Delta AOU = \left(1 - SS_{t0}\right)\Delta O_{2,sat} - O_{2,sat,t0}\,\Delta SS \qquad \text{(eq. S8)}$$

In this region, the first term, $(1–SS_{t0})\Delta O_{2,sat}$, is usually small at the annual scale (figure S2), and therefore the two approaches are largely equivalent.

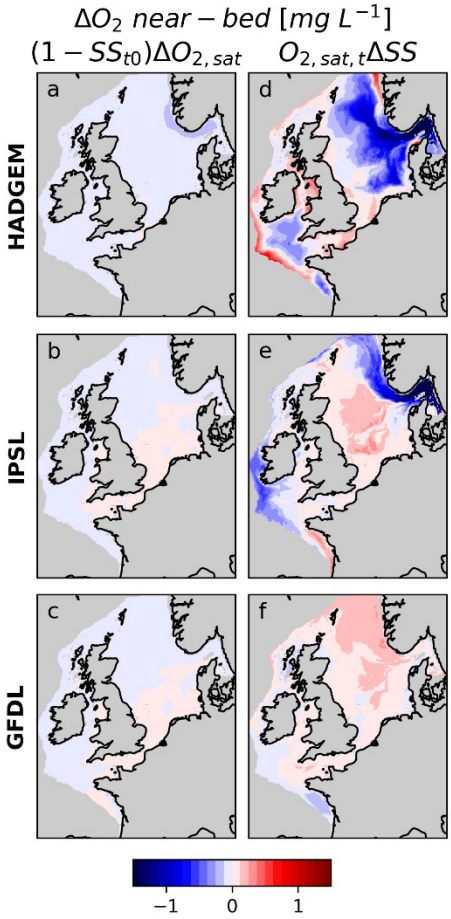

Figure S2: 30 years mean of the two terms constituting ΔAOU (from eq. 8)

115

120

125

130

135

140

145

S3. Present and future T, SAL, O_2, $O_{2,sat}$, SS.

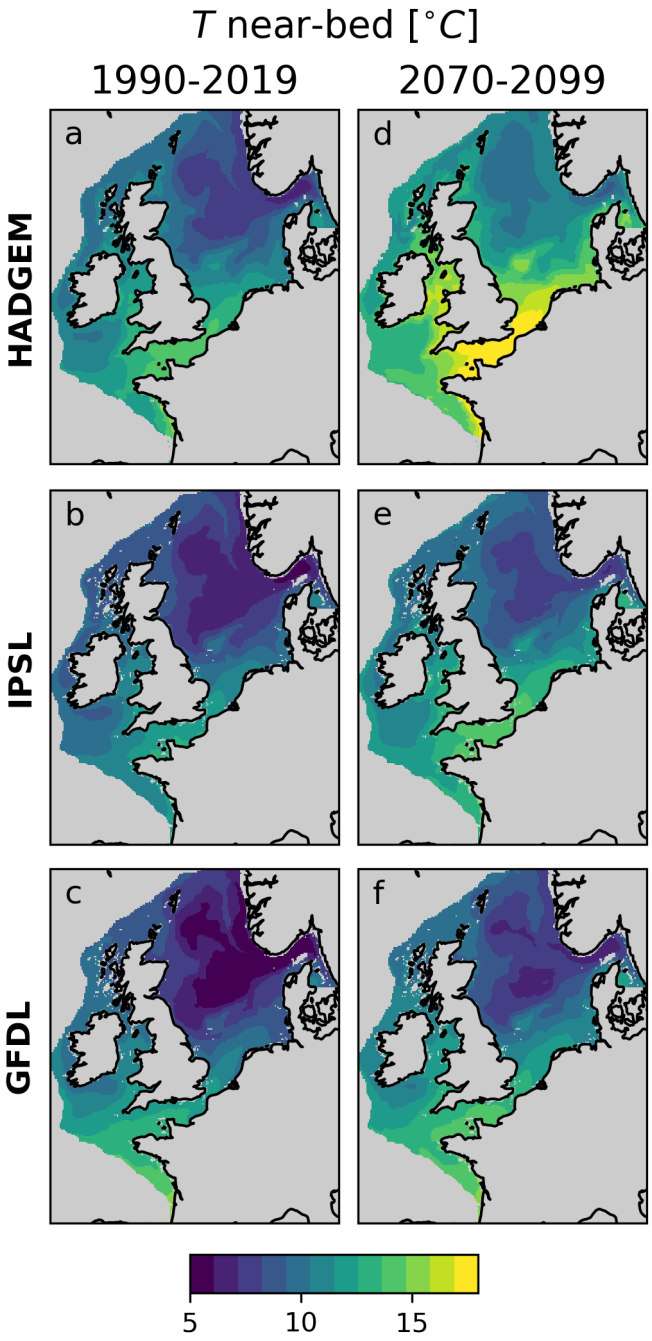

Fig. S3. Near-bed temperature (T) under present (mean of 1990-2019) and future (mean of 2070-2099) reference periods.

150

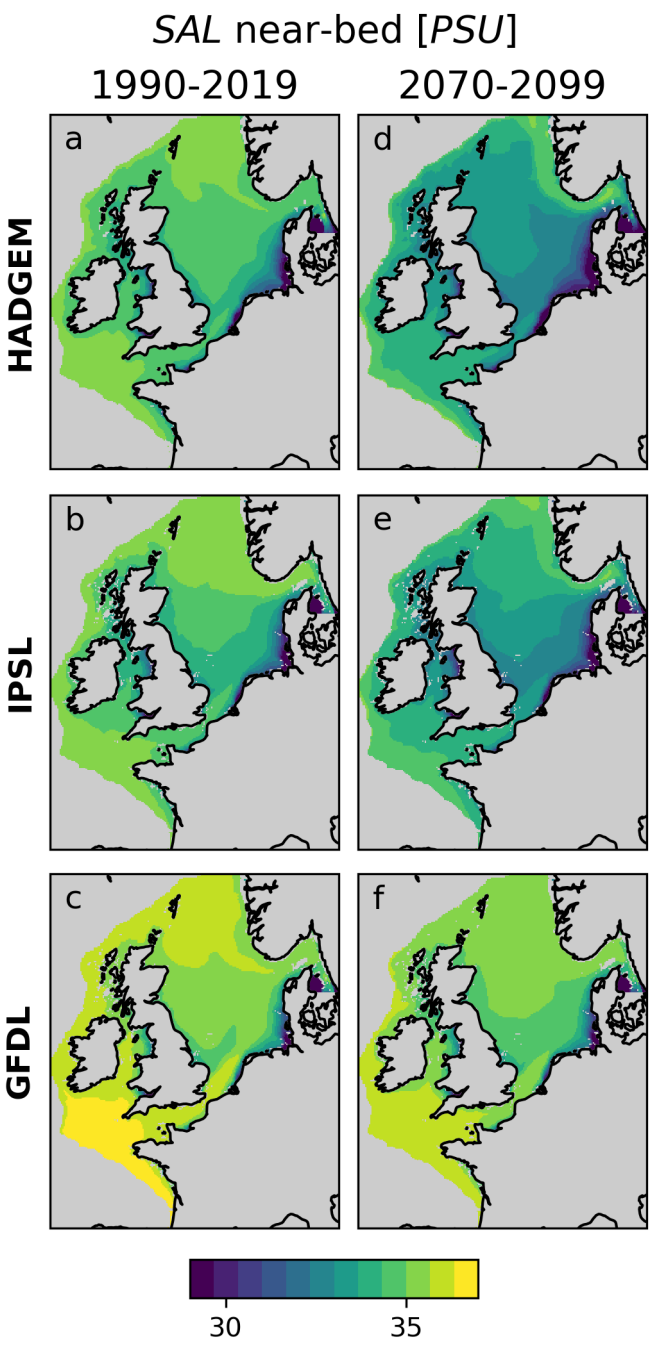

Fig. S4. Near-bed salinity (SAL) under present (mean of 1990-2019) and future (mean of 2070-2099) reference periods.

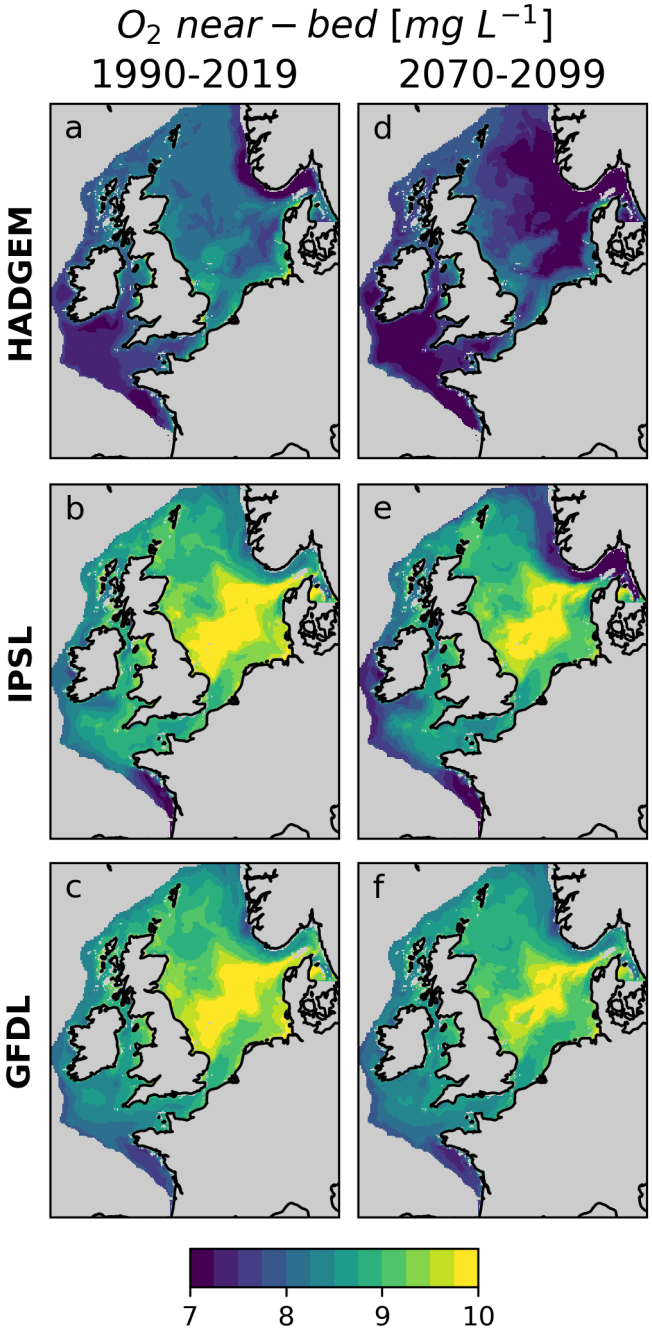

155 Fig. S5. Near-bed O_2 concentration under present (mean of 1990-2019) and future (mean of 2070-2099) reference periods.

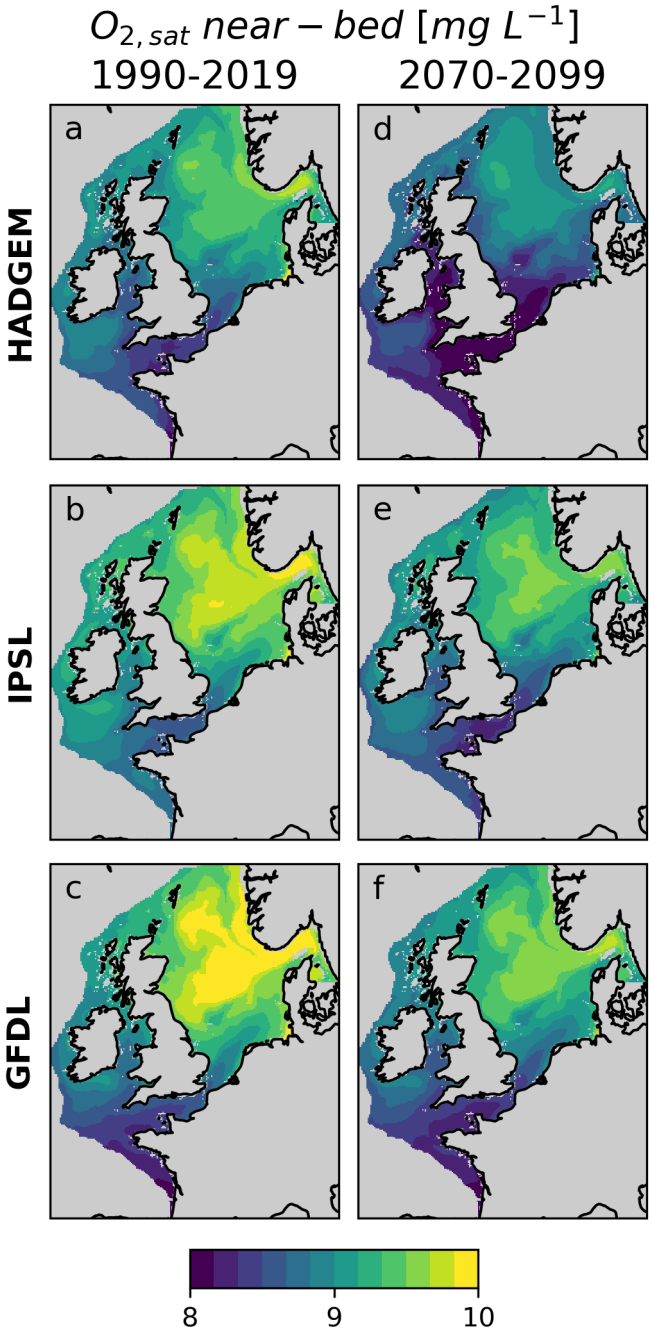

Fig. S6. Near-bed oxygen solubility ($O_{2,sat}$) under present (mean of 1990-2019) and future (mean of 2070-2099) reference periods.

160

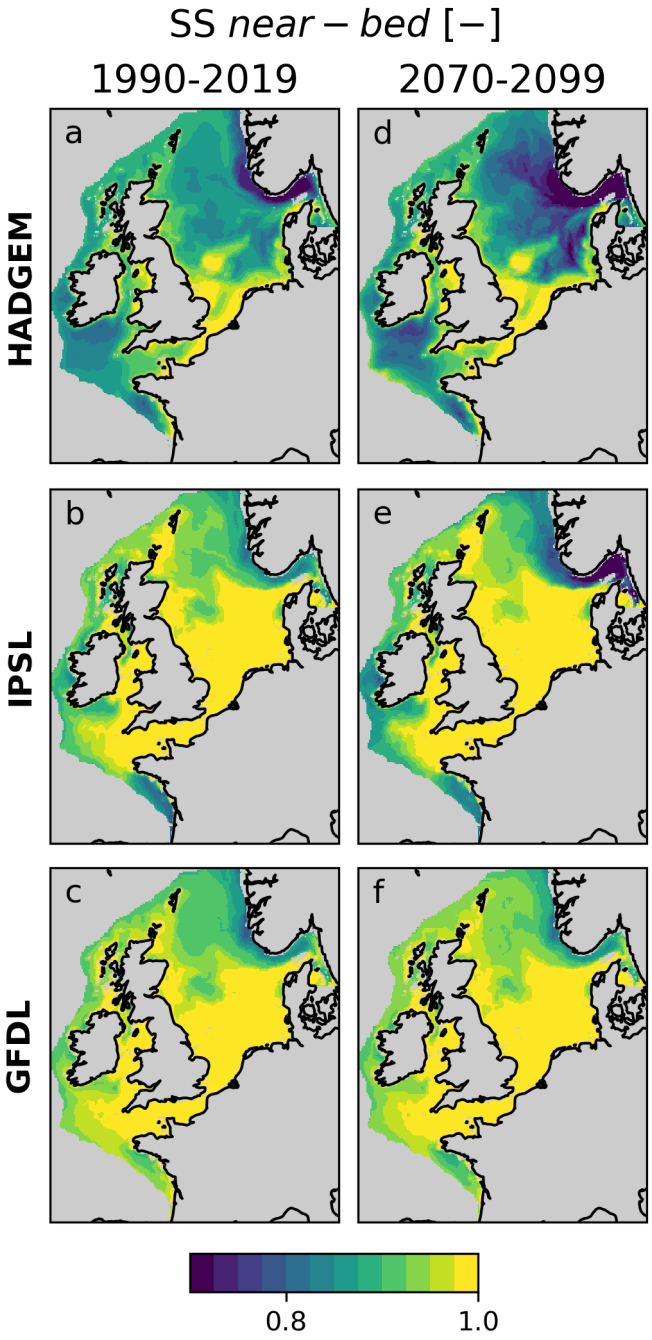

Fig. S7. Near-bed oxygen saturation state (SS) under present (mean of 1990-2019) and future (mean 2070-2099) reference periods.

165

References

Duteil, O., Koeve, W., Oschlies, A., Bianchi, D., Galbraith, E., Kriest, I., and Matear, R.: A novel estimate of ocean oxygen utilisation points to a reduced rate of respiration in the ocean interior, Biogeosciences, 10, 7723–7738, https://doi.org/10.5194/bg-10-7723-2013, 2013.

Hinrichs, I., Gouretski, V., Pätsch, J., Emeis, K.-C., and Stammer, D.: North Sea Biogeochemical Climatology (Version 1.1), , https://doi.org/10.1594/WDCC/NSBClim_v1.1, 2017.

Jolliff, J. K., Kindle, J. C., Shulman, I., Penta, B., Friedrichs, M. A. M., Helber, R., and Arnone, R. A.: Summary diagrams for coupled hydrodynamic-ecosystem model skill assessment, J. Mar. Syst., 76, 64–82, https://doi.org/10.1016/j.jmarsys.2008.05.014, 2009.

Sellar, A. A., Walton, J., Jones, C. G., Wood, R., Abraham, N. L., Andrejczuk, M., Andrews, M. B., Andrews, T., Archibald, A. T., Mora, L., Dyson, H., Elkington, M., Ellis, R., Florek, P., Good, P., Gohar, L., Haddad, S., Hardiman, S. C., Hogan, E., Iwi, A., Jones, C. D., Johnson, B., Kelley, D. I., Kettleborough, J., Knight, J. R., Köhler, M. O., Kuhlbrodt, T., Liddicoat, S., Linova□Pavlova, I., Mizielinski, M. S., Morgenstern, O., Mulcahy, J., Neininger, E., O'Connor, F. M., Petrie, R., Ridley, J., Rioual, J., Roberts, M., Robertson, E., Rumbold, S., Seddon, J., Shepherd, H., Shim, S., Stephens, A., Teixiera, J. C., Tang, Y., Williams, J., Wiltshire, A., and Griffiths, P. T.: Implementation of U.K. Earth System Models for CMIP6, J. Adv. Model. Earth Syst., 12, https://doi.org/10.1029/2019MS001946, 2020.

Yool, A., Palmiéri, J., Jones, C. G., De Mora, L., Kuhlbrodt, T., Popova, E. E., Nurser, A. J. G., Hirschi, J., Blaker, A. T., Coward, A. C., Blockley, E. W., and Sellar, A. A.: Evaluating the physical and biogeochemical state of the global ocean component of UKESM1 in CMIP6 historical simulations, Geosci. Model Dev., 14, 3437–3472, https://doi.org/10.5194/gmd-14-3437-2021, 2021.